Langmuir

Article

pubs.acs.org/Langmuir

Sequential Tasks Performed by Catalytic Pumps for Colloidal Crystallization

Ali Afshar Farniya,[†] Maria J. Esplandiu,*[,†,‡] and Adrian Bachtold[§]

[†]Institut Catala de Nanociencia i Nanotecnologia (ICN2), Campus Universitat Autònoma de Barcelona (UAB), 08193 Bellaterra, Barcelona, Spain

[‡]Consejo Superior de Investigaciones Científicas (CSIC), ICN2 Building, Campus Universitat Autònoma de Barcelona (UAB), 08193 Bellaterra, Barcelona, Spain

[§]Institut de Ciencies Fotoniques (ICFO), Mediterranean Technology Park, 08860 Castelldefels, Barcelona, Spain

Supporting Information

ABSTRACT: Gold−platinum catalytic pumps immersed in a chemical fuel are used to manipulate silica colloids. The manipulation relies on the electric field and the fluid flow generated by the pump. Catalytic pumps perform various tasks, such as the repulsion of colloids, the attraction of colloids, and the guided crystallization of colloids. We demonstrate that catalytic pumps can execute these tasks sequentially over time. Switching from one task to the next is related to the local change of the proton concentration, which modifies the colloid ζ potential and, consequently, the electric force acting on the colloids.

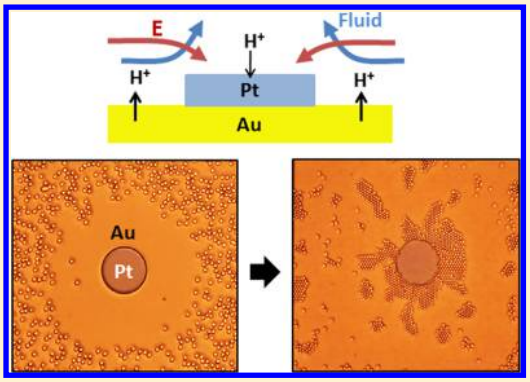

1. INTRODUCTION

In the last few years, there has been a growing interest in the study of active matter. These systems, which work far from equilibrium driven by a constant input of energy, exhibit various interesting and surprising phenomena, such as collective dynamics, complex self-organization, and the emergence of large-scale coherent structures.[1−12] Biology provides a wealth of archetypes of active systems that consume chemical energy to self-organize into complex structures and to perform different collective tasks. Some examples include cytoskeleton motors, self-propelled microorganisms, biofilm patterning, bacterial colonies,[13−26] and even at larger scales swarming phenomena, bird flocks, and fish schooling.[27−29] The tasks achieved by biological active systems are much more sophisticated than those of active systems fabricated thus far by humans.

Artificial swimmers, such as self-propelled active colloids and catalytic Janus particles, also provide nice examples of collective motility, swarming, and dynamic self-assembly.[1,3,5,6,8−11,30−44] Microfabricated catalytic pumps can be used to manipulate particles in solution and to form crystals of colloids.[45−50] These active swimmers and pumps are driven by catalytic reactions on their surface, which triggers electro-hydrodynamic forces.[5,8,30−52] The growth of colloidal crystals with swimmers and pumps is an interesting alternative to the more traditional colloidal self-assembly triggered by external fields.[53−64] However, artificial active systems have accomplished tasks that are rather simple thus far. Usually, artificial active systems effectuate only a single task that does not change in time in an autonomous way.

In this paper, we use microfabricated catalytic pumps to manipulate silica colloids by means of fluid flow and electric field. Interestingly, we have found that catalytic pumps can perform a sequence of different tasks over time. First, pump disks repel colloids far away. Second, pump disks direct colloids toward them. Third, pump disks assemble colloids in a crystal around them. We correlate the change between the first and second task to the variation of the proton concentration, which greatly affects the ζ potential of the colloids. The formation of the colloidal crystal is assisted by the electro-hydrodynamic forces of the pump. We observe how the colloids rearrange themselves in the crystal to heal defects.

2. EXPERIMENTAL SECTION

Catalytic pumps consist of 20−50 μm diameter Pt disks patterned on gold films. Pumps are fabricated using standard electron-beam lithography techniques. Pumps are subjected to 1 min of oxygen plasma cleaning (360 W) to remove residual poly(methyl methacrylate) (PMMA)/organic contamination and to activate the surface as reported before.[48] An 8 mm diameter and 0.12 mm thick gasket-like spacer (Invitrogen) is placed on top of the wafer patterned with micropumps. A 1 wt % hydrogen peroxide solution containing negatively charged colloids is added to the vacant space created by the

Received: August 5, 2014
Revised: September 5, 2014
Published: September 8, 2014

gasket. The wafer is immediately capped with a thin glass cover. The negative colloids are 1.5 μm diameter silica spheres (Kisker Biotech GmbH and Co.) with a ζ potential of −83.5 mV. The concentration of colloids is about 10^9 particles/mL. The motion of particles is optically recorded with a 5 frames/s rate and analyzed with the Diatrack software to determine their velocity. The ζ potential of the colloids and their variation in different pH solutions are carried out with a Zetasizer Nano-ZS (Malvern Instruments) based on electrophoretic light scattering.

3. RESULTS AND DISCUSSION

Hydrogen peroxide is used as the chemical input to trigger the catalytic actuation. The chemical fuel decomposes at both metal structures, with one of them acting as the anode and the other one acting as the cathode (Figure 1a).

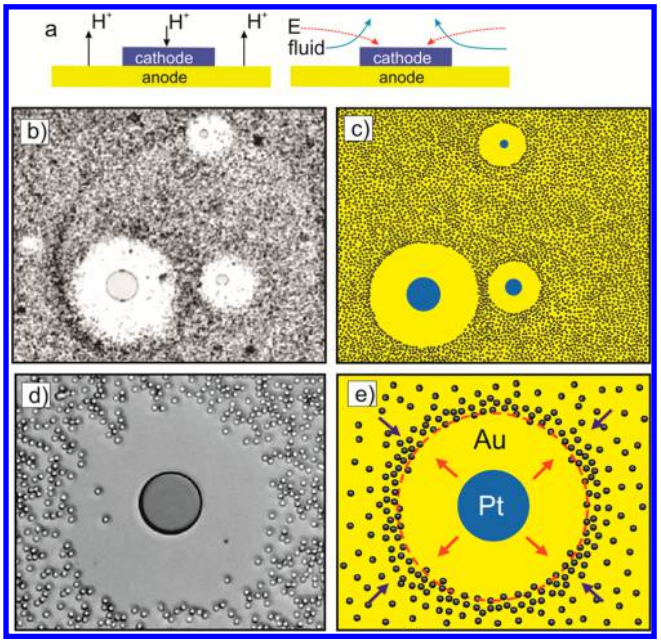

Figure 1. (a) Schematics representing the production and consumption of protons, the electric field line, and the fluid flow. (b–e) Optical microscopy images and schematics of pumps and colloids when H_2O_2 is put on the surface of the device. Colloids are repelled from the pump disk. In panel e, the red arrows indicate the electric force acting on the colloids, whereas the blue arrows indicate the fluid flow.

reaction at the anode

$$H_2O_2 \rightarrow O_2 + 2H^+ + 2e^- \quad (1)$$

reaction at the cathode

$$H_2O_2 + 2H^+ + 2e^- \rightarrow H_2O \quad (2)$$

Previous results demonstrated that oxygen plasma cleaning of the surface is mandatory to activate motion. Under these conditions, the platinum disk acts as the cathode and the gold surface acts as the anode in the presence of H_2O_2.[48] The electrochemical reaction generates an excess of protons at the anode, which is consumed at the cathode. As a result, an electric field pointing toward the Pt disk is generated, which drives a fluid flow in the same direction (Figure 1a).

The motion of colloids can be basically ascribed to two contributions, one coming from the electrophoretic force ($v_{eof} = \varepsilon E_r \zeta_c/\eta$) and the other one coming from the fluid flow (v_f). The fluid moves because of electro-osmosis, so that $v_f = -\varepsilon E_r \zeta_{Au}/\eta$. The radial velocity of colloids is given by

$$v_r = v_{eof} + v_f = \varepsilon E_r(\zeta_c - \zeta_{Au})/\eta \quad (3)$$

where E_r is the radial electric field, ε is the fluid permittivity, η is the fluid viscosity, and ζ_c and ζ_{Au} are the ζ potentials of the colloids and the Au surface. Previous measurements allowed us to estimate the ζ potential of the Au film ($\zeta_{Au} = -33$ mV).[48]

When H_2O_2 containing negatively charged silica colloids ($\zeta_c = -83.5$ mV) is placed onto catalytic micropumps, a region free of colloids forms around the Pt disk (panels b–e of Figure 1). Colloids remain more than 20 μm away from the disk edge. This region free of colloids is consistent with a strong radial electric force that repels negatively charged colloids from the pump disk.

However, this repulsive area is only formed at the very first stage of the experiment. Many other interesting features start emerging in time as is outlined in Figure 2. After the initial

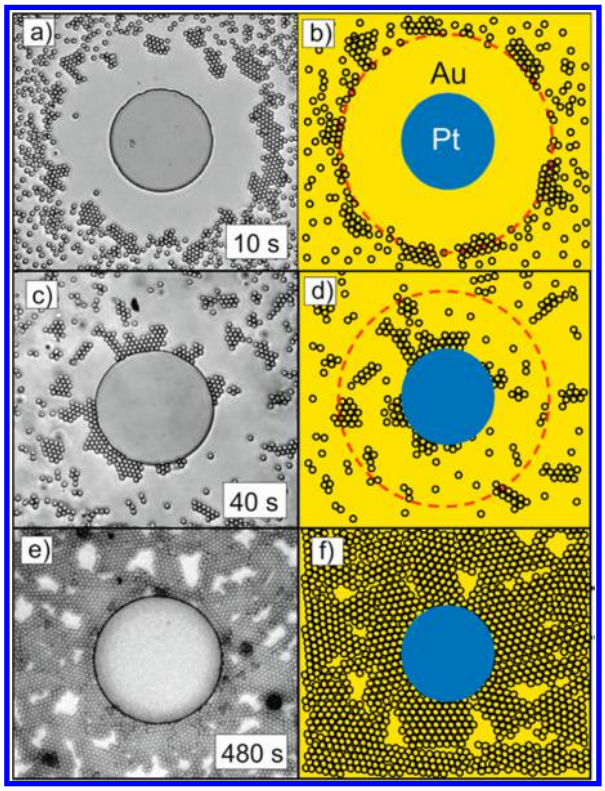

Figure 2. Optical microscopy images and schematics of pumps and colloids. (a and b) Cluster formation far away from the pump disk. (c and d) Motion of small clusters and individual colloids toward the pump disk. (e and f) Colloidal crystal formation around the pump disk.

repulsion, silica colloids start aggregating into small clusters (panels a and b of Figure 2). At the same time, these small clusters as well as individual colloids start moving toward the Pt disk (panels c and d of Figure 2). Once arrived at the pump disk, colloids assemble themselves in a crystal (panels e and f of Figure 2).

The formation of small clusters in panels a and b of Figure 2 is attributed to the production of protons at the Au surface. To show this, we fabricate Pt–Au micropumps patterned near a region with a silicon oxide surface (Figure 3a). Colloids do not assemble together in the region with the silicon oxide surface.

dx.doi.org/10.1021/la503118t | Langmuir 2014, 30, 11841–11845

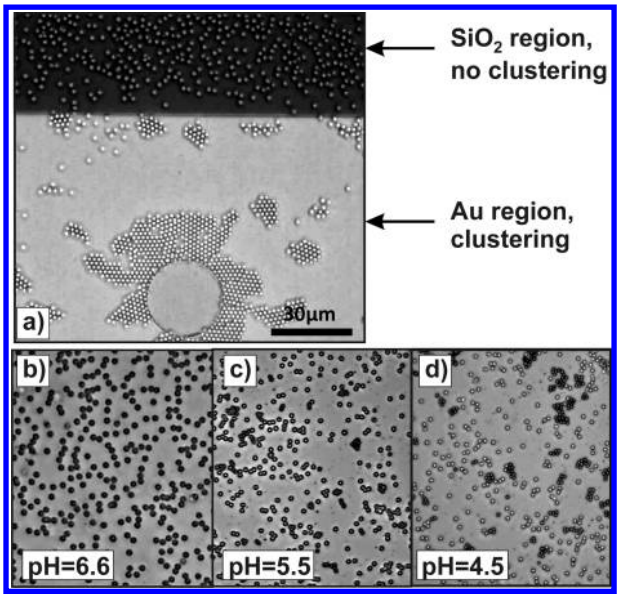

Figure 3. (a) Optical microscopy image of a micropump patterned near a region with a silicon oxide surface. (b–d) Optical snapshots of the dispersion of colloids at different pH values in the absence of hydrogen peroxide. The clustering occurs below a pH of around 5.5.

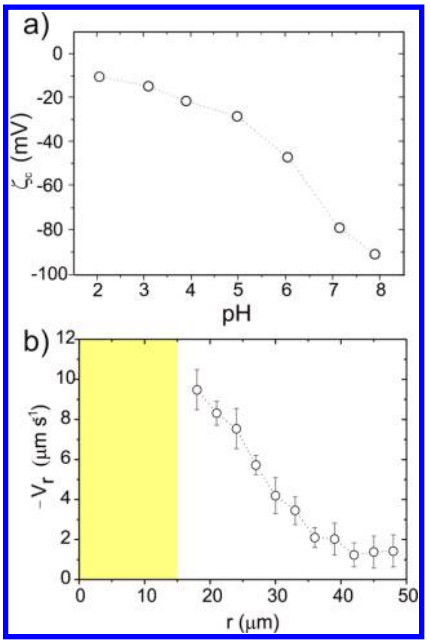

Figure 4. (a) Variation of the ζ potential of colloids as a function of pH. The measurements are performed by preparing different pH solutions in a 1 mM buffer phosphate. (b) Averaged radial velocity of colloids as a function of the radial coordinate *r*.

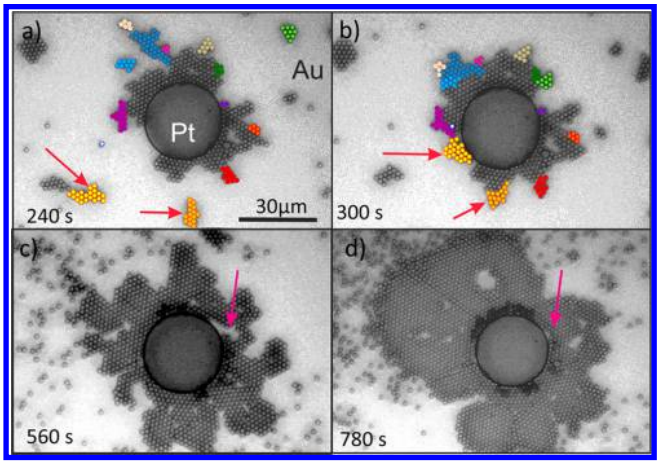

Figure 5. (a–d) Evolution of the colloidal crystal. In panels a and b, some incoming clusters are colored to show that their shape can change once they reach the crystal. In panels c and d, the arrows illustrate the defect healing effect. The darker zone just at the rim of the Pt disk in panel d corresponds to the region consisting of two layers of colloids.

They only feature Brownian motion. In contrast, the formation of clusters occurs over the gold surface, the region where protons are produced. This suggests that the cluster formation is correlated with the proton production. To gain more insight on this issue, we monitor the dispersion of colloids above a gold surface for different proton concentrations in the absence of hydrogen peroxide (panels b–d of Figure 3). Colloids do not assemble together at high pH, but they start to form small clusters at pH ≈ 5.5. This pH is close to the one estimated on the gold surface when the pump is actuated with H_2O_2.[48]

In Figure 4a, we measure the variation of the ζ potential of silica colloids as a function of pH. The colloid ζ potential becomes less negative upon decreasing the pH. Overall, all of these experiments indicate that the formation of small clusters is due to the change of the ζ potential of colloids subjected to the production of protons at the Au surface. Indeed, the continuous generation of protons at the surface might protonate the negative oxygen moieties of the silica, so that the charge of the colloid is reduced and the interaction between the colloids is promoted.

The motion of the colloids toward the pump disk in panels c and d of Figure 2 is attributed to the production of protons at the Au surface as well. Because of the change of the ζ potential induced by protons, the electric repulsion of the colloids from the pump disk is lowered, allowing colloids to move toward the disk. The radial velocity of colloids, obtained by averaging 10 different trajectories, increases as colloids approach the pump disk (Figure 4b). This increase of the velocity at the pump disk is similar to what was reported for positively charged colloids and quasi-neutral colloids.[48] This further supports the change of the ζ potential of silica colloids.

More than fascinating is the real-time monitoring of the colloidal self-assembly at the disk edge. The colloids stabilize at the edge of the pump disk, building a hexagonal crystal, which expands over the gold surface. The incoming small clusters change form and reorient themselves to better fit in the lattice of the growing colloidal crystal (red arrows in panels a and b of Figure 5). In addition, the defects of the crystal tend to disappear over time (arrows in panels c and d of Figure 5). These effects are attributed to the force from the moving fluid and the thermal energy that helps colloids find the more coordinated positions. We do not know at present the microscopic origin of why the colloidal crystal starts to grow from the edge of the Pt disk.

In these experiments, it is important to clean the pump surface with the oxygen plasma treatment. Without oxygen plasma treatment, we only observe the repulsion of the colloids from the pump disk; that is, the colloid clustering, the motion toward the pump disk, and the colloidal crystallization around the pump disk do not occur. This suggests that the oxygen plasma cleaning favors the production of protons when the pump is subjected to H_2O_2. Without oxygen plasma cleaning,

dx.doi.org/10.1021/la503118t | *Langmuir* 2014, 30, 11841–11845

the production of protons is weak and not enough to change significantly the ζ potential of colloids.

We also carry out experiments with positively charged particles (polystyrene spheres functionalized with amidine groups). The particles move toward the Pt disk, where they adsorb onto its surface.[48] The particles form a structure that is not well ordered. In other words, the particles do not form a colloidal crystal.

4. CONCLUSION

In this paper, we demonstrate the use of bimetallic catalytic pumps made of noble materials to guide colloidal crystallization at precise locations without the need of an external energy source. The local self-generated electro-hydrodynamic forces induced by electrochemical reactions together with the sensitivity of the colloid ζ potential to the local pH conditions are the basic ingredients for tailoring the colloidal crystal process. Silica colloids crystallize in a two-dimensional fashion through a series of sequential steps controlled by the proton concentration.

■ ASSOCIATED CONTENT

Supporting Information

Videos showing the different tasks performed by the catalytic micropumps. This material is available free of charge via the Internet at http://pubs.acs.org.

■ AUTHOR INFORMATION

Corresponding Author

*E-mail: mariajose.esplandiu@cin2.es.

Notes

The authors declare no competing financial interest.

■ ACKNOWLEDGMENTS

The authors acknowledge support from the European Union (ERC-carbonNEMS project), the Spanish government (FIS2009-11284, MAT2012-31338), and the Catalan government (AGAUR, SGR).

■ REFERENCES

(1) András, C.; Vicsek, T. Collective of interacting self-propelled particles. *Phys. A* **2000**, *281*, 17−29.
(2) Kruse, K.; Joanny, J. F.; Jüllicher, F.; Prost, J.; Sekimoto, K. Aster, vortices and rotating spirals in active gels of polar filaments. *Phys. Rev. Lett.* **2004**, *92*, 078101.
(3) Ramachandran, S.; Kumar, P. B. S.; Pagonabarraga, I. A lattice-Boltzmann model for suspensions of self-propelling coloidal particles. *Eur. Phys. J. E: Soft Matter Biol. Phys.* **2006**, *20*, 151−158.
(4) Schaller, V.; Weber, C.; Semmrich, C.; Frey, E.; Bausch, A. R. Polar patterns of driven filaments. *Nature* **2010**, *467*, 73−77.
(5) Palacci, J.; Cottin-Bizonne, C.; Ybert, C.; Bocquet, L. Sedimentation and effective temperature of active colloidal suspensions. *Phys. Rev. Lett.* **2010**, *105*, 088304.
(6) Enculescu, M.; Stark, H. Active colloidal suspensions exhibit polar order under gravity. *Phys. Rev. Lett.* **2011**, *107*, 058301.
(7) Köhler, S.; Schaller, V.; Bausch, A. R. Structure formation in active networks. *Nat. Mater.* **2011**, *10*, 462−468.
(8) Theurkauff, I.; Cottin-Bizonne, C.; Palacci, J.; Ybert, C.; Bocquet, L. Dynamic clustering in active colloidal suspensions with chemical signaling. *Phys. Rev. Lett.* **2012**, *108*, 268303.
(9) Farrell, F. D. C.; Marchetti, M. C.; Marenduzzo, D.; Tailleur, J. Pattern formation in self-propelled particles with density-dependent motility. *Phys. Rev. Lett.* **2012**, *108*, 248101.
(10) Bricard, A.; Caussin, J.B.; Desreumaux, N.; Dauchot, O.; Bartolo, D. Emergence of macroscopic directed motion in populations of motile colloids. *Nature* **2013**, *503*, 95−98.
(11) Palacci, J.; Sacanna, S.; Steinberg, A. P.; Pine, D. J.; Chaikin, P. M. Living crystals of light-activated colloidal surfers. *Science* **2013**, *339*, 936−940.
(12) Mognetti, B. M.; Saric, A.; Angioletti-Uberti, S.; Cacciuto, A.; Valeriani, C.; Frenkel, D. Living clusters and crystals from low-density suspensions of active colloids. *Phys. Rev. Lett.* **2013**, *111*, 245702.
(13) Czirók, A.; Ben-Jacob, E.; Cohen, I.; Vicsek, T. Formation of complex bacterial colonies via self-generated vortices. *Phys. Rev. E: Stat. Phys., Plasmas, Fluids, Relat. Interdiscip. Top.* **1996**, *54*, 1791−1801.
(14) Nedelec, F. J.; Surrey, T.; Maggs, A. C.; Leibler, S. Self-organization of microtubules and motors. *Nature* **1997**, *389*, 305−308.
(15) Desai, A.; Mitchison, T. J. Microtubule polymerization dynamics. *Annu. Rev. Cell Dev. Biol.* **1997**, *13*, 83−117.
(16) Howard, J. Molecular motors: Structural adaptations to cellular functions. *Nature* **1997**, *389*, 561−567.
(17) Brenner, M. P.; Levitov, L. S.; Budrene, E. O. Physical mechanisms for chemotactic pattern formation by bacteria. *Biophys. J.* **1998**, *74*, 1677−1693.
(18) Surrey, T.; Nedelec, F.; Leibler, S.; Karsenti, E. Physical properties determining self-organization of motors and microtubules. *Science* **2001**, *292*, 1167−1171.
(19) Dombrowski, C.; Cisneros, L.; Chatkaew, S.; Goldstein, R. E.; Kessler, J. O. Self-concentration and large scale coherence in bacterial dynamics. *Phys. Rev. Lett.* **2004**, *93*, 098103.
(20) Riedel, I. H.; Kruse, K.; Howard, J. A self-organized vortex array of hydrodynamically entrained sperm cells. *Science* **2005**, *309*, 300−303.
(21) Helenius, J.; Brouhard, G.; Kalaidzidis, Y.; Diez, S.; Howard, J. The depolymerizing kinesin MCAK uses lattice diffusion to rapidly target microtubule ends. *Nature* **2006**, *441*, 115−119.
(22) Loose, M.; Fischer-Friedrich, E.; Ries, J.; Kruse, K.; Schwille, P. Spatial regulators for bacterial cell division self-organize into surface waves in vitro. *Science* **2008**, *320*, 789−792.
(23) Fletcher, D. A.; Mullins, R. D. Cell mechanics and the cytoskeleton. *Nature* **2010**, *463*, 485−492.
(24) Gardner, M. K.; Charlebois, B. D.; Janosi, I. M.; Howard, J.; Hunt, A. J.; Odde, D. J. Rapid microtubule self-assembly kinetics. *Cell* **2011**, *146*, 582−592.
(25) Vignaud, T.; Blanchoin, L.; Thery, M. Directed cytoskeleton self-organization. *Trends Cell Biol.* **2012**, *22*, 671−682.
(26) Evans, L. D. B.; Poulter, S.; Terentjev, E. M.; Hughes, C.; Fraser, G. M. A chain mechanism for flagellum growth. *Nature* **2013**, *504*, 287−290.
(27) Grossman, D.; Aranson, I. S.; Ben Jacob, E. Emergence of agent swarm migration and vortex formation through inelastic collisions. *New J. Phys.* **2008**, *10*, 023036.
(28) Cavagna, A.; Cimarelli, A.; Giardina, I.; Parisi, G.; Santagati, R.; Stefanini, F.; Viale, M. Scale-free correlations in starling flocks. *Proc. Natl. Acad. Sci. U. S. A.* **2010**, *107*, 11865−11870.
(29) Katz, Y.; Tunstrom, K.; Ioannou, C. C.; Huepe, C.; Couzin, I. D. Inferring the structure and dynamics of interaction in schooling fish. *Proc. Natl. Acad. Sci. U. S. A.* **2011**, *108*, 18720−18725.
(30) Ibele, M.; Mallouk, T. E.; Sen, A. Schooling behavior of light-powered autonomous micromotors in water. *Angew. Chem., Int. Ed.* **2009**, *48*, 3308−3312.
(31) Hong, Y.; Velegol, D.; Chaturvedi, N.; Sen, A. Biomimetic behavior of synthetic particles: From microscopic randomness to microscopic control. *Phys. Chem. Chem. Phys.* **2010**, *12*, 1423−1435.
(32) Hong, Y.; Diaz, M.; Córdova-Figueroa, U. M.; Sen, A. Light-driven titanium dioxide based reversible microfireworks and micromotor/micropump systems. *Adv. Funct. Mater.* **2010**, *20*, 1−9.
(33) Pumera, M. Electrochemically powered self-propelled electrophoretic nanosubmarines. *Nanoscale* **2010**, *2*, 1643−1649.
(34) Kagan, D.; Balasubramanian, S.; Wang, J. Chemically triggered swarming of gold microparticles. *Angew. Chem., Int. Ed.* **2011**, *50*, 503−506.

(35) Duan, W.; Ibele, M.; Liu, R.; Sen, A. Motion analysis of light-powered autonomous silver chloride nanomotors. *Eur. Phys. J. E: Soft Matter Biol. Phys.* **2012**, *35*, 77.
(36) Yan, J.; Bloom, M.; Bae, S. C.; Luitjen, E.; Granick, S. Linking synchronization to self-assembly using magnetic Janus colloids. *Nature* **2012**, *491*, 578−581.
(37) Solovev, A. A.; Sanchez, S.; Schmidt, O. G. Collective behavior of self-propelled catalytic micromotors. *Nanoscale* **2013**, *5*, 1284−1293.
(38) Duan, W.; Liu, R.; Sen, A. Transition between collective behaviors of micromotors in response to different stimuli. *J. Am. Chem. Soc.* **2013**, *135*, 1280−1273.
(39) Wang, W.; Duan, W.; Sen, A.; Mallouk, T. E. Catalytically powered dynamic assembly of rod-shaped nanomotors and passive tracer particles. *Proc. Natl. Acad. Sci. U. S. A.* **2013**, *110*, 17744−17749.
(40) Gao, W.; Pei, A.; Feng, X. M.; Hennessy, C.; Wang, J. Organized self-assembly of Janus micromotors with hydrophobic hemispheres. *J. Am. Chem. Soc.* **2013**, *135*, 998−1001.
(41) Baraban, L.; Harazim, S. M.; Sanchez, S.; Schmidt, O. G. Chemotactic behavior of catalytic motors in microfluidic channels. *Angew. Chem., Int. Ed.* **2013**, *52*, 5552−5556.
(42) Wang, H.; Zhao, G. J.; Pumera, M. Beyond platinum: Bubble-propelled micromotors based on Ag and MnO_2 catalysts. *J. Am. Chem. Soc.* **2014**, *136*, 2719−2722.
(43) Guix, M.; Mayorga-Martinez, C. C.; Merkoci, A. Nano/micromotors in (bio)chemical science applications. *Chem. Rev.* **2014**, *114*, 6285−6322.
(44) Soler, L.; Sanchez, S. Catalytic nanomotors for environmental monitoring and water remediation. *Nanoscale* **2014**, *6*, 7175−7182.
(45) Kline, T. R.; Paxton, W. F.; Wang, Y.; Velegol, D.; Mallouk, T. E.; Sen, A. Catalytic micropumps: Microscopic convective fluid flow and pattern formation. *J. Am. Chem. Soc.* **2005**, *127*, 17150−17151.
(46) Kline, T. R.; Iwata, J.; Lammert, P. E.; Mallouk, T. E.; Sen, A.; Velegol, D. Catalytically driven colloidal patterning and transport. *J. Phys. Chem. B* **2006**, *110*, 24513−24521.
(47) Subramanian, S.; Catchmark, J. M. Control of catalytically generated electroosmotic fluid flow through surface zeta potential engineering. *J. Phys. Chem. C* **2007**, *111*, 11959−11964.
(48) Afshar Farniya, A.; Esplandiu, M. J.; Reguera, D.; Bachtold, A. Imaging the proton concentration and mapping the spatial distribution of the electric field of catalytic micropumps. *Phys. Rev. Lett.* **2013**, *111*, 168301.
(49) Punckt, C.; Jan, L.; Jiang, P.; Frewen, T. A.; Saville, D. A.; Kevrekidis, I. G.; Aksay, I. A. Autonomous colloidal crystallization in a galvanic microreactor. *J. Appl. Phys.* **2012**, *112*, 074905.
(50) Jan, L.; Punckt, C.; Khusid, B.; Aksay, I. A. Directed motion of colloidal particles in a galvanic microreactor. *Langmuir* **2013**, *29*, 2498−2505.
(51) Solovev, A. A.; Sanchez, S.; Mei, Y.; Schmidt, O. G. Tunable catalytic tubular micro-pumps operating at low concentrations of hydrogen peroxide. *Phys. Chem. Chem. Phys.* **2011**, *13*, 10131−10133.
(52) Zhao, G.; Wang, H.; Sanchez, S.; Schmidt, O. G.; Pumera, M. Artificial micro-cinderella based on self-propelled micromagnets for the active separation of paramagnetic particles. *Chem. Commun.* **2013**, *49*, 5147−5119.
(53) Trau, M.; Saville, D. A.; Aksay, I. A. Field-induced layering of colloidal crystals. *Science* **1996**, *272*, 706−708.
(54) Giersig, M.; Mulvaney, P. Preparation of ordered colloid monolayers by electrophoretic deposition. *Langmuir* **1993**, *9*, 3408−3413.
(55) Solomontsev, Y.; Böhmer, M.; Anderson, J. L. Particle clustering and pattern formation during electrophoretic deposition: A hydrodynamic model. *Langmuir* **1997**, *13*, 6058−6068.
(56) Yeh, S.; Seul, M.; Shralman, B. I. Assembly of ordered colloidal aggregates by electric-field-induced fluid flow. *Nature* **1997**, *386*, 57−59.
(57) Solomontsev, Y.; Guelcher, S. A.; Bevan, M.; Anderson, J. L. Aggregation dynamics for two particles during electrophoretic deposition under steady fields. *Langmuir* **2000**, *16*, 9208−9216.
(58) Zhang, K.; Liu, X. Y. In situ observation of colloidal monolayer nucleation driven by an alternating electric field. *Nature* **2004**, *429*, 739−743.
(59) Bigioni, T. P.; Lin, X.; Nguyen, T. T.; Corwin, E. I.; Witten, T. A.; Jaeger, H. M. Kinetically driven self-assembly of highly ordered nanoparticle monolayers. *Nat. Mater.* **2006**, *5*, 265−270.
(60) Liu, Y.; Liu, X.; Narayanan, J. Kinetics and equilibrium distribution of colloidal assembly under an alternating electric field and correlation to degree of perfection of colloidal crystals. *J. Phys. Chem. C* **2007**, *111*, 995−998.
(61) Ristenpart, W. D.; Aksay, I. A.; Saville, D. A. Electrically driven flow near a colloidal particle close to an electrode with a faradaic current. *Langmuir* **2007**, *23*, 4071−4080.
(62) Sapozhnikov, M. V.; Tolmachev, Y. V.; Aranson, I. S.; Kwok, W. K. Dynamic self-assembly an patterns in electrostatically driven granular media. *Phys. Rev. Lett.* **2003**, *90*, 114301.
(63) Aranson, I. S.; Sapozhnikov, M. V. Theory pattern formation of metallic microparticles in poorly conducting liquids. *Phys. Rev. Lett.* **2004**, *92*, 234301.
(64) Bartlett, A. P.; Agarwal, A. K.; Yethiraj, A. Dynamic templating of colloidal patterns in three dimensions with nonuniform electric fields. *Langmuir* **2011**, *27*, 4313−4318.